Published in final edited form as:
Exp Dermatol. 2011 April ; 20(4): 339–345. doi:10.1111/j.1600-0625.2011.01247.x.

SOX2 and nestin expression in human melanoma: an immunohistochemical and experimental study

Alvaro C. Laga[1], **Qian Zhan**[1], **Carsten Weishaupt**[2], **Jie Ma**[3], **Markus H. Frank**[3], and **George F. Murphy**[1]

[1]Department of Pathology, Program in Dermatopathology, Brigham and Women's Hospital, Harvard Medical School, Eugene Braunwald Research Center, Boston, MA, USA

[2]Department of Dermatology, University of Münster, Münster, Germany

[3]Transplantation Research Center, Children's Hospital Boston and Brigham and Women's Hospital, Harvard Medical School, Boston, MA, USA

Abstract

SOX2 is an embryonic neural crest stem-cell transcription factor recently shown to be expressed in human melanoma and to correlate with experimental tumor growth. SOX2 binds to an enhancer region of the gene that encodes for nestin, also a neural progenitor cell biomarker. To define further the potential relationship between SOX2 and nestin, we examined co-expression patterns in 135 melanomas and 37 melanocytic nevi. Immunohistochemical staining in 27 melanoma tissue sections showed an association between SOX2 positivity, spindle cell shape and a peripheral nestin distribution pattern. In contrast, SOX2-negative cells were predominantly epithelioid, and exhibited a cytoplasmic pattern for nestin. In tissue microarrays, co-expression correlated with tumor progression, with only 11% of nevi co-expressing SOX2 and nestin in contrast to 65% of metastatic melanomas, and preliminarily, with clinical outcome. Human melanoma lines that differentially expressed constitutive SOX2 revealed a positive correlation between SOX2 and nestin expression. Experimental melanomas grown from these respective cell lines in murine subcutis and dermis of xenografted human skin maintained the association between SOX2-positivity, spindle cell shape, and peripheral nestin distribution. Moreover, the cytoplasmic pattern of nestin distribution was observed in xenografts generated from SOX2-knockdown A2058 melanoma cells, in contrast to the periperhal nestin pattern seen in tumors grown from A2058 control cells transfected with non-target shRNA. In aggregate, these data further support a biologically significant linkage between SOX2 and nestin expression in human melanoma.

Keywords

melanoma; nestin; SOX2; stem cell

Correspondence: George F. Murphy, MD, Program in Dermatopathology, EBRC-401, 221 Longwood Ave., Boston, MA 02115, USA, Tel.: (617) 525-7485, Fax: (617) 264-5149, gmurphy@rics.bwh.harvard.edu.

Supporting Information

Additional Supporting Information may be found in the online version of this article:

Figure S1. e-supplement. (k–n) Representative tissue microarray cores showing SOX2 (nuclear brown) and nestin (cytoplasmic blue-black) double staining. k, negative for both SOX2 and nestin (background); l, nestin-positive; m, SOX2-positive; n, Co-positive (k–n, ×100). (O) Kaplan–Meier curve showing a significant difference in survival distribution ($P = 0001$) when comparing patients with nestin and SOX2 co-positive melanomas (group 1) to patients with SOX2-only, nestin-only or conegative melanomas (group 0).

Please note: Wiley-Blackwell are not responsible for the content or functionality of any supporting materials supplied by the authors. Any queries (other than missing material) should be directed to the corresponding author for the article.

Introduction

Nestin is an intermediate filament protein expressed by migrating and proliferating neural crest stem cells during embryogenesis (1). Terminal cell differentiation is associated with loss of immunoreactivity for nestin, and in mature tissues, nestin expression is primarily restricted to areas of regeneration (2,3). Although the precise physiological function and regulation of nestin remain unclear, it is generally accepted that it is a biomarker of multilineage progenitor cells, and its expression may indicate pluripotency and regenerative potential (2). In human skin, nestin expression has been reported in hair follicle progenitor cells and epidermal stem cells that may differentiate into adipocytes, fibrocytes and neurons (4–6). However, one recent study documented nestin immunoreactivity and mRNA only in the periappendageal mesenchyme, but not in the epithelium (including the bulge region of hair follicles), and thus proposed a strictly intramesenchymal location of nestin expression in human scalp (7).

In human neoplasia, nestin expression has positively correlated with histologic grade in human gliomas, gastrointestinal stromal tumors (GIST), and angiosarcomas (8,9). Moreover, nestin has been documented by immunohistochemistry in melanocytic tumors, where both the frequency and intensity of expression positively correlate with tumor progression and decreased survival (10–15). Flamminger et al. recently showed that SOX9 and SOX10 are required for nestin expression in human melanoma (16). A follow-up study by the same investigators demonstrated that expression of nestin with SOX9 and SOX10 by immunohistochemistry in human melanomas correlated with advanced tumor stage and ulceration (17). Thus, the co-expression of SOX-family transcription factors with nestin may serve as an indicator of melanoma virulence.

We recently documented that SOX2, an embryonic stem-cell transcription factor also of neural crest stem-cell lineage, is expressed in melanoma and relates to melanoma tumorigenic growth *in vivo* (18). Of interest, an enhancer region on the nestin gene dependent on the binding of SOX2 has been previously reported (19). Accordingly, the aim of the present study was to investigate whether a relationship exists between SOX2 and nestin expression in patient-derived and experimentally induced melanomas. The data indicate that distinctive cytological characteristics and nestin distribution are associated with SOX2 expression, and that these molecules may interact in a manner that relates to melanoma growth and virulence.

Materials and methods

Human samples

Paraffin-embedded sections of 27 human melanomas and 21 non-dysplastic nevi were obtained from the Department of Pathology, Brigham and Women's Hospital according to an approved Institutional Review Board (IRB) protocol. Two tissue microarrays (TMA) representing 135 melanomas and 22 non-dysplastic nevi, both annotated according to primary versus metastatic melanoma origin, and one annotated with survival outcomes (n = 59) were evaluated (Cat. No. ME1003, US Biomax Inc., Rockville, MD, USA and Cat. No. IMH-369, Imgenex, San Diego, CA, USA). Tissue microarray cores are defined as 0.6–1.0 mm cylindrical tissue samples as provided by manufacturers. Cores not fully represented for melanoma or nevus or not immunohistochemically evaluable due to artifact were excluded from analysis.

Cell lines and cell growth *in vitro*

To better understand the potential relationship between SOX2 and nestin in an *in vivo* system, human melanoma cells were cultured to subsequently generate xenograft tumors.

Human melanoma cell lines A2058 and SK-MEL-5 were obtained from American Type Culture Collection (Manassas, VA, USA) and grown in Dulbecco's modified Eagle's medium (DMEM; Sigma-Aldrich Inc., St Louis, MO, USA) supplemented with 10% inactivated fetal bovine serum (FBS; Hyclone laboratories Inc., Logan, UT, USA), 200 m_M/l $_L$-glutamine, 100 IU/ml penicillin and 100 μg/ml streptomycin, and maintained at 37°C in a humidified atmosphere containing 5% CO_2. Briefly, subconfluent cultures were trypsinized and seeded in 35-mm wells at 1×10^4 cells per well. Cells were re-fed twice weekly. At given intervals, cells in quadruplicate wells were harvested and counted in a Coulter counter (Coulter Electronics, Luton, UK).

Real time RT-PCR

Total RNA from human melanoma cell lines (listed above) was extracted using the RNAeasy Mini Kit (Qiagen, Valencia, CA, USA). Total RNA was reverse-transcribed to cDNA using the SuperScript III First-strand Synthesis System for RT-PCR. cDNA from all four cell lines (detailed above) was surveyed for SOX2 and nestin expression using the SOX2 (Cat. No. Hs01053049-s1) and nestin (Cat. No. Hs00707120-s1) assays for real time RT-PCR (Applied Biosystems, Foster City, CA, USA). The glyceraldehyde-3-phosphate dehydrogenase housekeeping gene was used for normalization and data were analysed using the $2^{-\Delta\Delta C_t}$ method (20).

SOX2 knockdown in A2058 melanoma cells by lentiviral short hairpin RNA

Recombinant lentiviral vectors were generated by co-transfecting pLKO.1-shSOX2 (Sigma) harboUring short hairpin RNA for human SOX2, or pLKO.1 scramble, containing non-target control shRNA (Addgene) with psPAX2, pMD2. G into 293T cells using calcium phosphate according to manufacturer's instructions (Sigma). Culture supernatant containing recombinant lentiviral particles was harvested 48 h post-transfection and used to infect A2058 melanoma cells. Twenty-four hours after infection, cells were selected with 1 μg/ml of puromycin for 3 days.

Western blotting

Subconfluent cell cultures were washed with PBS and extracted in lysis buffer (1% Triton X-100, 1% deoxycholic acid, 2 mmol/l $CaCl_2$, 1.8 mg/ml iodoacetamide and 1 mmol/l phenylmethyl sulfonyl fluoride in PBS). Cell lysates were quantified with a bicinchinonic acid protein assay kit (Pierce, Rockford, IL, USA). An equal amount of protein (50 μg) from each sample was subjected to electrophoresis on NuPAGE 4% to 12% Bis–Tris gels (Invitrogen, Carlsbad, CA, USA), transblotted onto nitrocellulose membranes (Pierce), and probed with primary anti-SOX2 (Cell Signaling Techonology, Danvers, MA, USA), or anti-nestin (Millipore, Billerica, MA, USA) antibodies, followed by a peroxidase-conjugated secondary antibody (Pierce). Subsequent re-probing using anti β-actin (Abcam, Cambridge, MA, USA) was performed as an internal loading control. Immunoreactive bands were detected using super-Signal West Femto Chemiluminescent substrate (Pierce), captured by a Syngene Chemi Genius Bio Imaging System (Syngene, Frederick, MD, USA), and quantified by densitometry. Experiments were performed in duplicate with consistency.

Human melanoma xenotransplantation

Subconfluent melanoma cells from melanoma cell lines, as well as A2058-SOX2-KD and A2058-scramble (control) cells were suspended in serum-free medium at a concentration of 10^8 cells/ml in PBS. One hundred microlitres of cell suspension (10^7 cells) were injected subcutaneously into dorsal skin of recipient nonobese diabetic/severe combined immunodeficiency mice (C.B17; Taconic Laboratory, Germantown, NY, USA; five mice per condition). Mice were maintained under defined conditions according to institutional

guidelines and approved experimental protocol. Tumor formation and growth were assessed throughout the duration of the experiment or until tumor burden or disease state required euthanasia as defined by the approved protocol. Representative sections containing the greatest tumor cross-sectional area and thus best approximating the size of the generally spherical to ovoid tumor nodules were evaluated.

Human melanoma xenotransplantation to human skin chimeric mice

Human to chimeric mouse/human skin melanoma xenotransplantation was performed. Single donor-derived split human skin was obtained after IRB approval by cutting discarded abdominal skin with a 0.016-inch gauge dermatome and grafted onto immunodeficient $Rag2^{-/-}$ mice according to a protocol approved by the institutional animal committee, as previously described (21). Briefly, two 1.5 cm^2 graft beds were established on the dorsum of 4- to 8-week-old $Rag2^{-/-}$ mice. Mice were prophylactically treated with one additional tablet of food containing 3 mg of amoxicillin, 0.69 mg of metronidazole and 0.185 mg of bismuth to prevent H. pylorii infection. Human skin was trimmed to fit to the graft-bed and held in place by staples for 10 days after surgery. A2058 or SK-MEL-5 melanoma cells (2×10^6) were injected intra-dermally into human skin grafts 6 weeks after xenotransplantation. Skin grafts were harvested in entirety 3 weeks after tumor cell inoculation, fixed in formalin, paraffin-embedded and serially sectioned and stained with H&E using standard methods. Representative sections containing the greatest tumor cross-sectional area and thus best approximating the size of the generally spherical to ovoid tumor nodules were evaluated. The experiments were performed in triplicate and median estimated tumor volumes are presented.

Immunohistochemistry

Five micrometre sections were deparaffinized in xylene, followed by treatment in 100% ethanol, 95% and 75% ethanol, and by serial hydration using dH_2O. Then, sections were placed in 1× target retrieval solution (Dako, Carpenteria, CA, USA) and boiled in a Pascal pressure chamber (Dako) at 125°C for 30 s, 90°C for 10 s, and then allowed to cool down to room temperature. Immunohistochemistry was performed using a two-step horseradish peroxidase method. Briefly, the sections were first incubated with primary antibodies at 4°C overnight. The following primary antibodies were used: goat anti-human SOX2 (Neuromics, Edina, MN, USA) and mouse anti-human nestin (Millipore). After washing out unbound primary antibodies with tris-buffered saline-0.05% Tween 20 (TBST), the tissue sections were incubated with peroxidase conjugated secondary antibody at room temperature for 30 min, and then washed with TBST 5 min three times. Immunoreactivity was detected using NovaRed peroxidase substrate (Vector Laboratories, Burlingame, CA, USA).

For double-labelled immunohistochemical staining, sections were deparaffinized and heat-induced antigen retrieval with Target Retrieval Solution (Dako) was used. Sections were incubated with SOX2 antibody (Neuromics) and nestin (Millipore) at room temperature for 1 h and then with peroxidase conjugated horse antigoat antibody (Vector) and Alkaline phosphatase (AP)-conjugated horse anti-mouse antibody at room temperature for 30 min. SOX2 was detected with NovaRed peroxidase substrate (Vector). Nestin staining was detected with nitro blue tetrazolium chloride/5-bromo-4-chloro-3-indolyl phosphate, toluidine salt alkaline phosphatase (NBT/BCIP AP) substrate (Hoffman-La Roche, Nutley, NJ, USA). Immunoreactivity in patient tumor whole sections and tissue microarray cores was designated positive when unequivocal nuclear or cytoplasmic labeling was detected in >10% of the cells, for SOX2 and nestin, respectively. The pattern (localization) of staining was also recorded for all cases. Two independent observers blinded to all clinical and pathological data evaluated all cases.

Statistical analysis

The chi-squared or Fisher's exact test were used to determine significance in the difference of immunopositivity frequency distributions, as appropriate. The Wilcoxon signed-rank test was used to test for significance in the levels of SOX2 and nestin in melanoma cell lines. Survival analysis was performed using the Kaplan–Meier method, and the log-rank test was used for statistical significance. In all cases, the threshold for statistical significance was considered as a P-value < 0.05.

Results

Nestin and SOX2 expression in patient melanomas

Three of 21 nevi (14%) were positive for SOX2, and none showed immunoreactivity for nestin. As shown in Table 1, there were no melanomas positive only for SOX2 in this cohort. Thirteen melanomas (48%) were positive for both SOX2 and nesitn, with no significant difference between primary and metastatic tumors (10/21 primary and 3/5 metastatic), and 13 additional (48%) melanomas were immunoreactive for nestin only. There were no primary or metastatic melanomas negative for both SOX2 and nestin in this initial survey sample. Of interest, the pattern of nestin immunoreactivity was significantly different in SOX2-positive melanomas from that in SOX2-negative melanomas. Of 13 melanomas with strong nuclear immunoreactivity for SOX2, 12 showed a peripheral pattern of nestin immunoreactivity, whereas one case showed diffuse cytoplasmic reactivity. Of 13 SOX2-negative melanomas, nine showed diffuse cytoplasmic immunoreactivity for nestin, whereas four demonstrated a peripheral pattern (Fig. 1, chi-squared test: $P = 0.001$). The remaining case ($n = 1$) showed dichotomous spindle and epithelioid vertical growth phase morphology, with the spindle cell component exhibiting strong nuclear SOX2-positivity and a peripheral nestin pattern, and the epithelioid component being negative for SOX2, and showing diffuse nestin cytoplasmic reactivity (Fig. 1a–j). SOX2-positive cells with a peripheral pattern of nestin expression tended to be spindle-shaped, whereas SOX2-negative cells with a diffuse pattern of nestin expression tended to have a rounded, epithelioid morphology.

To further define nestin and SOX2 expression in a larger sample of biospecimens, two additional TMAs containing collectively 16 evaluable cores of non-dysplastic melanocytic nevi, 78 evaluable cores of primary melanoma and 30 evaluable cores of metastatic melanoma were examined. Tissue microarray cores are defined as 0.6–1.0 mm cylindrical tissue samples as provided by manufacturers. Cores not fully represented for melanoma or nevus or not immunohistochemically evaluable because of artifact were excluded from analysis. As shown in Table 1, only a minority of nevi (6%) were co-positive for both SOX2 and nestin, whereas 49% of primary melanomas and 70% of metastatic melanomas co-expressed both biomarkers. Correlation of nestin immunoreactivity patterns with nuclear SOX2 positivity or negativity was not possible in TMAs because of small size of sample cores.

One of the two TMAs analysed was annotated with survival outcomes and was comprised of 59 melanomas, 49 of which were evaluable (33 primary and 16 metastatic). Ten melanomas were excluded from analysis as a result of technically suboptimal (non-evaluable) cores. Of the evaluable cores, six (12%) were positive for SOX2 only (Figure S1m) and six (12%) were positive for nestin only (Figure S1l). Thirty-five cores (72%) were co-positive for SOX2 and nestin (Figure S1n, e-suplement), and the remaining two cores (4%) were negative for both SOX2 and nestin (Figure S1k). No significant relationship was found between SOX2 or nestin-only positivity and survival. However, a statistically meaningful association was observed when comparing tumors that co-expressed both SOX2 and nestin

with tumors that did not (SOX2-only positive, nestin-only positive, and negative for both SOX2 and nestin). Patients with co-positive tumors ($n = 35$) showed a significantly shorter survival than patients without co-positivity ($n = 14$, log-rank test: $P = 0.0001$, Figure S1o). To eliminate the possibility that the observed difference in survival between the two groups may be driven by an imbalance in stage amongst patients with metastatic disease (e.g. patients with more advanced metastatic disease in one group), we repeated the analysis only in patients with primary melanoma. In this group, we also observed a statistically significant difference in survival between patients with co-positive primary melanomas ($n = 22$) and patients without co-positivity ($n = 11$, log-rank test: $P < 0.0001$).

Nestin and SOX2 expression in human melanoma cell lines

To further define the relationship between nestin and SOX2 expression in human melanomas, we investigated mRNA and protein levels of both in two human melanoma cell lines by real time RT-PCR and western blot. The A2058 and SK-MEL-5 cell lines were used because of their differential expression of SOX2 (~250-fold difference). As shown in Fig. 2, mRNA and protein levels of both SOX2 and nestin are significantly higher in A2058 cells than in SK-MEL-5 cells (Wilcoxon, $P < 0.001$). These findings were consistent in both cultured melanoma cells from the indicated lines, and in tumor xenografts generated from them (data not shown).

Patterns of nestin and SOX2 expression in human melanoma xenograft tumors

We next utilized melanoma xenograft tumors generated in immunodeficient mice from the A2058 and SK-MEL-5 melanoma cell lines. Tumors xenografted subcutaneously generated with A2058 melanoma cells showed a predominantly spindle cell morphology, while tumors derived from SK-MEL-5 cells displayed a predominantly epithelioid morphology (Fig. 3). Both A2058 and SK-MEL-5-derived tumors grew as well-demarcated, non-infiltrative tumor nodules. In keeping with *in vitro* data, A2058-derived xenografts showed strong nuclear immunoreactivity for SOX2, whereas SK-MEL-5 tumors were negative. Nestin immunoreactivity was observed in both cases (A2058 and SK-MEL-5 xenograft tumors), although the pattern of reactivity was distinct for each, with A2058 (SOX2-positive) tumors showing a peripheral pattern of reactivity, as compared with SK-MEL-5 (SOX2-negative) tumors demonstrating a diffuse cytoplasmic pattern.

Because the host microenvironment and related epigenetic factors relevant to the murine subcutis may potentially influence these results in an *in vivo* bioassay, we replicated these experiments utilizing a human-skin mouse chimeric model. This approach involved the grafting of normal adult human skin onto the backs of immunodeficient mice. Human skin 6 weeks after xenotransplantation retained a human cutaneous immunohistochemical profile. A2058 and SK-MEL-5 cells generated viable intra-dermal tumors that were sampled and evaluated after 4 weeks.

Tumors derived from A2058 cells were composed predominantly of plump fusiform cells that expressed nuclear SOX2 and a peripheral nestin pattern (Fig. 4). Moreover, tumors derived from A2058 melanoma cells had an infiltrative perimeter, in contrast to homologous tumors grown in murine subcutis. By contrast, tumors formed from the SK-MEL-5 line were comprised predominantly of rounded, epitheliod cells devoid of SOX2 and expressing nestin in a diffuse cytoplasmic pattern. Additionally, tumors derived from SK-MEL-5 cells had well-demarcated, non-infiltrative perimeters. Thus, tumor expression profiles of SOX2 and nestin in the humanized skin xenografts confirmed observations in the subcutaneous model and in patient melanomas, and further disclosed a tendency for infiltration of the human dermis by tumors derived from A2058, but not SK-MEL-5, melanoma lines.

Effect of SOX2 expression on *in vivo* nestin patterning

To investigate whether SOX2 expression contributes to nestin patterning, we generated stable A2058-SOX2-KD clones with 90% efficiency. As shown in Fig. 5, SOX2-KD melanoma cells and xenograft tumors generated from them showed an increase in nestin mRNA and protein, in the order of 66% at the protein level. By immunohistochemistry, tumor xenografts derived from SOX2-KD melanoma cells are negative for SOX2 and show a strong cytoplasmic distribution of nestin. In contrast, A2058 control cells transfected with non-target shRNA and corresponding xenograft tumors show strong nuclear positivity for SOX2 and cytoplasmic positivity for nestin in a peripheral distribution pattern, similar to that seen in wild type A2058 melanoma cells. Of interest, knockdown of nestin in A2058 melanoma cells did not change significantly the levels of SOX2 mRNA and protein (data not shown).

Discussion

The expression of nestin in melanocytic tumors, with incremental frequency of immunoreactivity in melanomas compared with nevi, has been previously documented (10–15). Tanaka and coworkers showed that synergistic interactions between group B1 (SOX1/2/3)/group C (SOX11) SOX and class III POU transcription factors within the nucleus determine nestin expression and may play a regulatory role in neural primordial stem cells. Accordingly, in the present study we investigated in melanocytic tumors the relationship of the expression of nestin and SOX2, a SOX-family member recently implicated in melanoma virulence (18). Nestin and SOX2 were expressed only in a minority of nevi, but they are expressed in the majority of melanomas. Overall, 48% of primary melanoma samples and 69% of metastatic melanoma samples analysed in this study co-expressed both biomarkers, and an exploratory analysis of the potential clinical significance indicates a significantly shorter survival for patients with melanomas co-expressing nestin and SOX2. It should be emphasized however, that these findings will need confirmation in a larger dataset, as our analysis was limited by lack of clinical–pathological information relevant to melanoma prognosis other than melanoma-specific survival times (22). Although no melanomas negative for both nestin and SOX2 were evident in whole tissue sections, we observed a decreasing trend for co-negative tumors with disease progression, with no co-negative metastatic tumors in the two TMAs analysed. The discrepancy between whole sections and TMA cores may be explained in part by the error incurred when single cores are sampled for a TMA to represent the entire tumor block, and by selection bias inherent to convenience samples.

Melanoma whole sections showed a distinct pattern of nestin immunoreactivity in SOX2-positive melanoma cells as compared to SOX2-negative cells. SOX2-positive cells generally showed peripheral nestin immunoreactivity, while SOX2-negative cells showed a diffuse cytoplasmic pattern. Although we could not explore this observation with rigor in the TMAs because of the small sample core size, we were able to replicate this finding in two experimental murine models using human melanoma cell lines. SOX2-positive tumors generated from the A2058 melanoma cell line had higher levels of nestin and SOX2 mRNA and protein, and a peripheral pattern of nestin immunoreactivity. Tumors generated from SK-MEL-5 cells had significantly lower levels of SOX2 and nestin mRNA and protein, but showed a diffuse cytoplasmic nestin pattern. Importantly, the difference in nestin immunoreactivity pattern observed in a subset of patient melanomas and xenograft tumors generated from two different cell lines, could be induced in A2058 melanoma cells by knockdown of SOX2 (Fig. 5). Moreover, in this experimental setting, SOX2 knockdown was associated with increased levels of nestin by real time RT-PCR and western blot (Fig. 2).

Although the function of nestin remains poorly understood, nestin expression is enriched in a variety of cancers including melanoma, particularly in advanced and metastatic tumors, arguing for a role in cancer progression (8–15). A recent study showed that nestin is expressed in androgen-independent human prostatic carcinoma, and nestin gene knockdown in human prostate cancer cell lines inhibited *in vitro* migration and invasion without affecting cell growth. Moreover, the same study documented that nestin knockdown diminished metastasis fivefold compared with controls, while not affecting tumorigenicity at the inoculation site in a murine model (23). These findings are not surprising given that nestin is an intermediate filament, and tumor metastasis requires that a non-motile, quiescent cell transforms into a fibroblastoid phenotype capable of invasion, dissemination and growth at a distant site (24). This process resembles the epithelial-mesenchymal transition (EMT) that occurs physiologically during embryogenesis, regeneration and wound healing, and is accompanied by global cellular changes including replacement and redistribution of intermediate filament types (24). Although EMT is thought to be a major determinant of melanoma metastasis (25–27), whether nestin and/or SOX2 participate in such phenomena remains to be determined. However, it is intriguing to speculate that the different patterns observed reflect a change in nestin distribution, with the peripheral pattern, which is also associated with increased nestin mRNA and protein expression, conferring a more motile (mesenchymal) phenotype, and the diffuse cytoplasmic pattern associated with a more ‘non-motile (epithelioid) phenotype’ (28–30).

Nestin has been associated with clinical aggressiveness. In this study, SOX2 knockdown enhances nestin expression, and yet decreased survival is only associated with SOX2 *and* nestin expression. Although increased nestin expression has been previously shown to be associated with melanoma virulence (8–17), these studies did not control for concomitant expression of SOX2. In this study, we do not identify nestin alone as a virulence marker, raising the possibility that the previous studies may have been confounded by not including relevant cofactors that may be required to fully assess the independent biological effect of nestin expression. The fact that experimentally, SOX2 knockdown is associated with upregulation of nestin does not contradict the prospect that cellular aberrations whereby both are increased promote enhanced virulence. In previous work (18), the expression of SOX2 correlated with tumor growth in xenografts. Because knockdown of SOX2 inhibited growth, it is plausible that upregulation of nestin, an intermediate filament protein implicated in cell migration and metastasis (23), could be a compensatory mechanism to maintain tumor virulence despite diminution in SOX2 transcription. In such a model, those cells overexpressing both SOX2 and nestin would be anticipated to be most aggressive. Further studies to better identify these complex interrelationships in clinical context are therefore indicated.

Cell migration is a complex process that involves the formation of lamellopodia through polymerization of actin and sequential formation and disassembly of focal adhesion complexes (31,32). Studies indicate that intermediate filament proteins are involved in cell migration. It has been shown that increasing vimentin levels promote motility and metastatic potential (33,34). Moreover, intermediate filament proteins such as synemin, which is structurally similar to nestin, can bind to vinculin and actinin and in turn participate in cell movement through interactions with focal adhesions and actin (35). Accordingly, the association of a peripheral nestin pattern with a SOX2-positive, more spindle-shaped melanoma cell with increased potential for stromal infiltration could relate to functional participation of nestin in the migratory process.

In the study by Tanaka et al. (19), two groups of nestin-positive neural primordial cells within the embryonic nervous system were characterized: those expressing SOX2 and class III POU (e.g. Brn2) transcription factors and those expressing SOX11 and class III POU

transcription factors. The former cell subpopulation localized to the ventricular zone and characterized cells in a proliferative state, whereas the latter localized to the subventricular region and characterized a non-proliferative compartment, suggesting a major change in transcriptional regulation as cells shift from one compartment to the other. We have previously shown that SOX2 is expressed in human melanomas and it relates to tumorigenic growth *in vivo* (18). Recent studies have shown that SOX2 is an amplified gene in lung, esophageal and oral squamous cell carcinomas that functions as a lineage-survival oncogene (36–39). Whether nestin and SOX2 interact or synergize in melanoma cells is now open to question, and further studies including single and double gene 'knock-down' approaches, are required to investigate this hypothesis.

In conclusion, we show that nestin and SOX2 are co-expressed in a major subset of human melanomas, and that SOX2 expression correlates with distinctive patterns of nestin distribution. The preliminary data presented here raise the possibility that the SOX2/nestin-positive phenotype may confer greater clinical virulence. Whether this relates to local factors (cell proliferation, migration and invasion) or tendency for metastatic dissemination requires further study. The recognition, however, of a possible regulatory interaction between these two molecules that may define functional or prognostic parameters of melanoma behavior, paves the way for future investigations linking embryonic neural crest transcription factors and intermediate filaments with clinical course and outcome.

Supplementary Material

Refer to Web version on PubMed Central for supplementary material.

Acknowledgments

The authors wish to express their gratitude to Drs Yufei Xu and Yujiang Shi for their help with the SOX2-knockdown experiments.

Funding

This work was supported by the following grants from the National Institutes of Health: P50 CA93683, P30 AR42689, R01 CA138231, R01 CA113796. Dr Laga is supported by an Institutional Ruth L. Kirchenstein National Research Service Award (T32).

References

1. Lendahl U, Zimmerman LB, McKay RDG. Cell. 1990; 60:585–595. [PubMed: 1689217]
2. Wiese C, Rolletschek A, Kania G, et al. Cell Mol Life Sci. 2004; 61:2510–2522. (review). [PubMed: 15526158]
3. Ehrmann J, Kolar Z, Mokry J. J Clin Pathol. 2005; 58:222–223. [PubMed: 15677549]
4. Sellheyer K, Krahl D. J Am Acad Dermatol. 2010; 63:93–113. [Epub ahead of print]. [PubMed: 19864043]
5. Sellheyer K, Krahl D. J Cutan Pathol. 2010; 37:624–634. [PubMed: 20002239]
6. Li L, Mignone J, Yang M, et al. Proc Natl Acad Sci USA. 2003; 100:9958–9961. [PubMed: 12904579]
7. Tiede S, Kloepper JE, Ernst N, et al. J Invest Dermatol. 2009; 129:2711–2720. [PubMed: 19554024]
8. Veseleska R, Kuglik P, Cepjek P, et al. BMC Cancer. 2006; 6:32–43. [PubMed: 16457706]
9. Yang XH, Wu QL, Yu XB, et al. J Clin Pathol. 2008; 61:467–473. [PubMed: 17873113]
10. Brychtova S, Fiuraskova M, Hlobilková TB, et al. J Cutan Pathol. 2007; 34:370–375. [PubMed: 17448190]
11. Florenes VA, Holm R, Myklebost O, et al. Cancer Res. 1994; 54:354–356. [PubMed: 8275467]
12. Klein WM, Wu BP, Zhao S, et al. Modern Pathol. 2007; 20:102–107.

13. Piras F, Perra MT, Murtas D, et al. Oncol Rep. 2010; 23:17–24. [PubMed: 19956860]
14. Tanabe K, Amoh Y, Kanoh M, et al. Eur J Dermatol. 2010; 20:283–288. [PubMed: 20156773]
15. Fusi A, Ochsenreither S, Busse A, et al. Br J Dermatol. 2010; 163:107–114. [PubMed: 20346020]
16. Flamminger A, Besch R, Cook AL, et al. J Invest Dermatol. 2009; 129:945–953. [PubMed: 18923447]
17. Bakos RM, Maier T, Besch R, et al. Exp Dermatol. 2010; 19:e89–e94. [PubMed: 19845757]
18. Laga AC, Lai CY, Zhan Q, et al. Am J Pathol. 2010; 176:903–913. [PubMed: 20042675]
19. Tanaka S, Kamachi Y, Tanouchi A, et al. Mol Cell Biol. 2004; 24:2923–2931. [PubMed: 15024080]
20. Livak KJ, Schmittgen TD. Methods. 2001; 25:402–408. [PubMed: 11846609]
21. Juhasz I, Albelda SM, Elder DE, et al. Am J Pathol. 1993; 143:528–537. [PubMed: 8342600]
22. Bollschweiler E. Langenbecks Arch Surg. 2003; 344:239–244. [PubMed: 12920602]
23. Kleeberger W, Bova GS, Nielsen ME, et al. Cancer Res. 2007; 67:9199–9206. [PubMed: 17909025]
24. Huang S, Ingber DE. Breast Disease. 2006–2007; 26:27–54. (review).
25. Alonso SR, Tracey L, Ortiz P, et al. Cancer Res. 2007; 67:3450–3460. [PubMed: 17409456]
26. Yang J, Price MA, Li GY, et al. Cancer Res. 2009; 69:7538–7547. [PubMed: 19738072]
27. Na YR, Seok SH, Kim DJ, et al. Cancer Sci. 2009; 100:2218–2225. [PubMed: 19735263]
28. Ingber DE. Semin Cancer Biol. 2008; 18:356–364. (review). [PubMed: 18472275]
29. Ingber DE, Dike L, Hansen L, et al. Int Rev Cytol. 1994; 150:173–224. (review). [PubMed: 8169080]
30. Ingber DE. J Cell Sci. 1993; 104:613–627. (review). [PubMed: 8314865]
31. Webb DJ, Parsons JT, Horwitz AF. Nat Cell Biol. 2002; 4:97–100.
32. Yamaguchi H, Wyckoff J, Condeelis JM, et al. Curr Opin Cell Biol. 2005; 17:229–564.
33. Gilles C, Polette M, Zahm JM, et al. J Cell Sci. 1999; 112:4615–4625. [PubMed: 10574710]
34. Hendrix MJ, Seftor EA, Chu YW, et al. Cancer Metastasis Rev. 1996; 15:507–525. [PubMed: 9034607]
35. Doyle KL, Khan M, Cunningham AM. J Compar Neurol. 2001; 437:186–195.
36. Bass AJ, Watanabe H, Mermel CH, et al. Nat Genet. 2009; 41:1238–1242. [PubMed: 19801978]
37. Hussenet T, Dali S, Exinger J, et al. PLoS ONE. 2010; 5:e8960. [PubMed: 20126410]
38. Yuan P, Kadara H, Behrens C, et al. PLoS ONE. 2010; 5:e9112. [PubMed: 20161759]
39. Feier K, Knoepfle K, Flechtenmacher C, et al. Genes Chromosom Cancer. 2010; 49:9–16. [PubMed: 19787784]

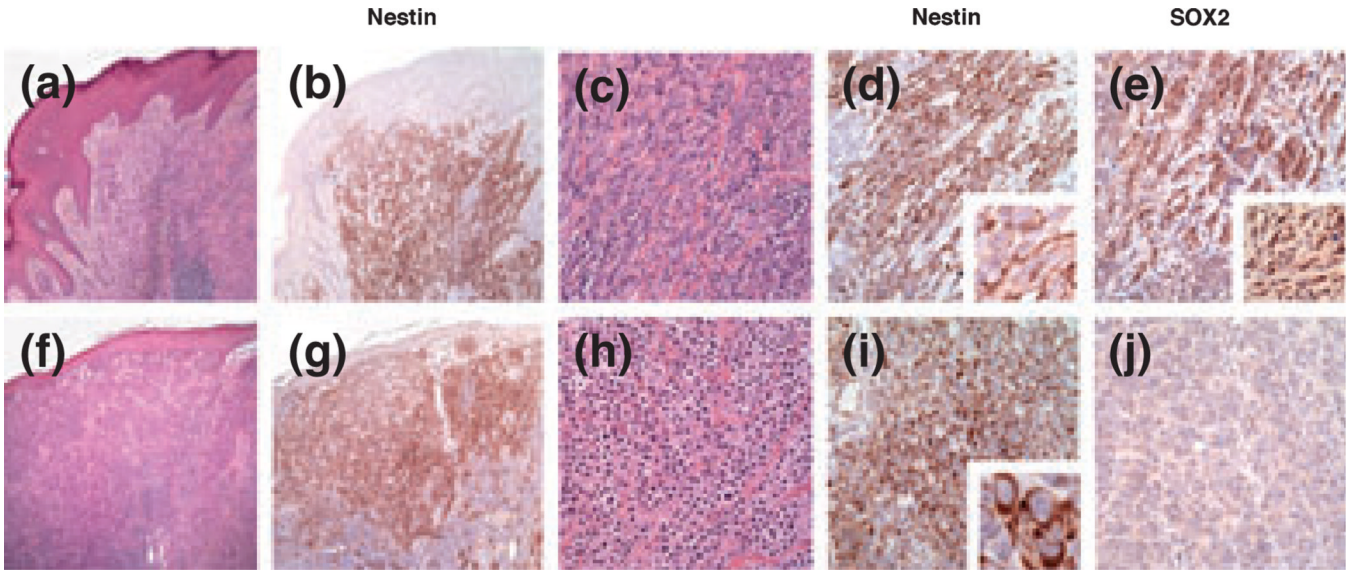

Figure 1.

SOX2 and nestin immunoreactivity in human melanoma. (a) Spindle cell morphology in part of a biphasic (spindle and epithelioid) melanoma [haematoxilin and eosin (H&E), ×40]. (b) The spindle cell component is immunoreactive for nestin (nestin, ×40). (c, d) The pattern of nestin immunoreactivity is predominantly peripheral (c: H&E, ×200; d: nestin, ×400; inset: ×1000). (e) Cells with peripheral immunoreactivity for nestin show nuclear SOX2 positivity (SOX2, ×200; inset: ×400). (f, g) Epithelioid cell morphology in part of a biphasic (spindle and epithelioid) melanoma (f: H&E, ×40; g: nestin, ×40). (h, i) The epitheliod cell component is also immunoreactive for nestin, but the pattern of immunoreactivity is diffuse cytoplasmic (h: H&E, ×200; i: nestin, ×200; inset: ×1000). (j) Cells with diffuse cytoplasmic immunoreactivity for nestin are negative for SOX2 (SOX2, ×200).

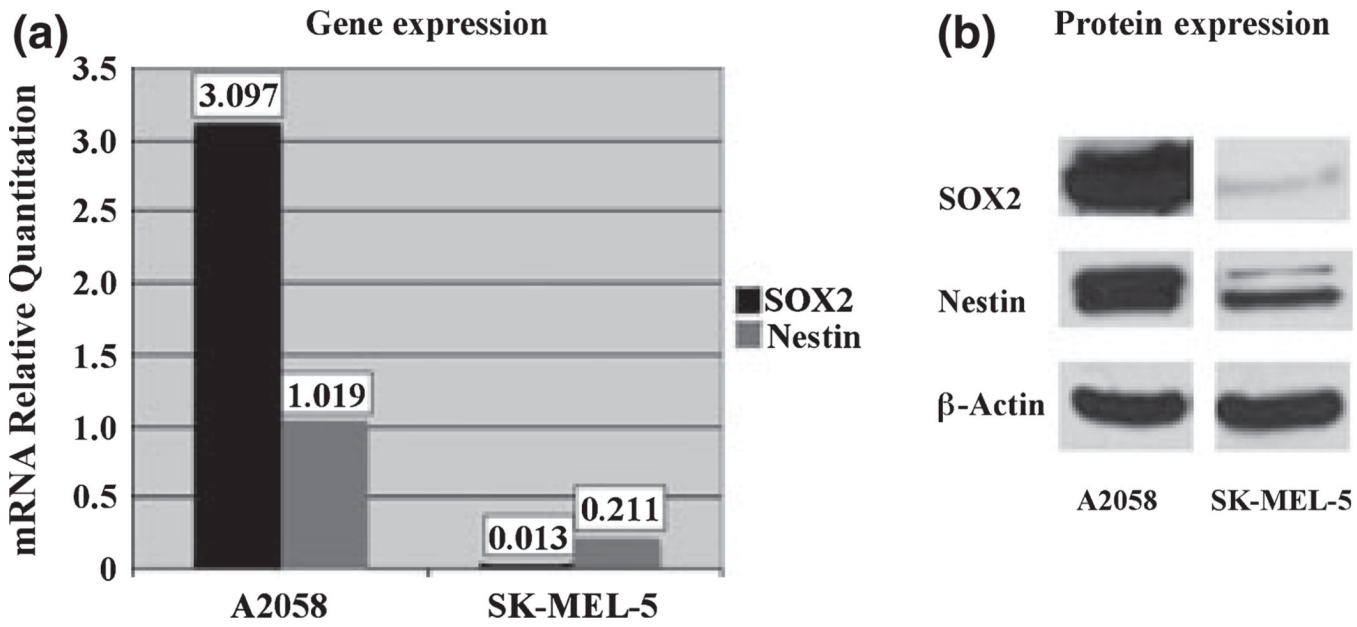

Figure 2.

Comparison of mRNA and protein levels of SOX2 and nestin in A2058 and SK-MEL-5 melanoma cell lines. A2058 melanoma cells have significantly higher mRNA (a) and protein (b) levels of SOX2 (black bars) and nestin (grey bars), relative to SK-MEL-5 melanoma cells ($P < 0.001$).

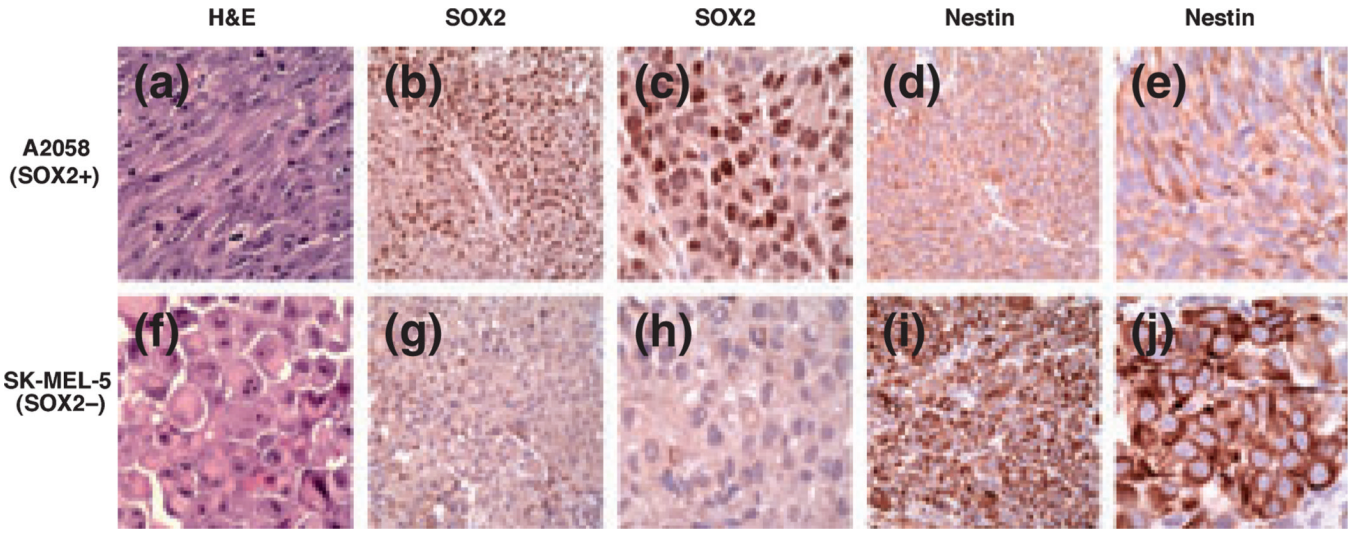

Figure 3.

Nestin and SOX2 immunoreactivity in cell line-derived subcutaneous human melanoma xenografts. (a) A2058-derived melanomas grow predominantly as spindle cell tumors (H&E, ×400). (b, c) A2058 melanoma xenograft tumors show strong nuclear immunoreactivity for SOX2 (b: ×200; c: ×400), with peripheral nestin immunoreactivity (d: ×200; e: ×400). (f) SK-MEL-5-derived melanoma xenografts grow predominantly as formed by rounded epitheliod cells (H&E, ×400). (g, h) In contrast, SK-MEL-5 melanomas are negative for SOX2, and show diffuse cytoplasmic immunoreactivity for nestin (i: ×200; j: ×400).

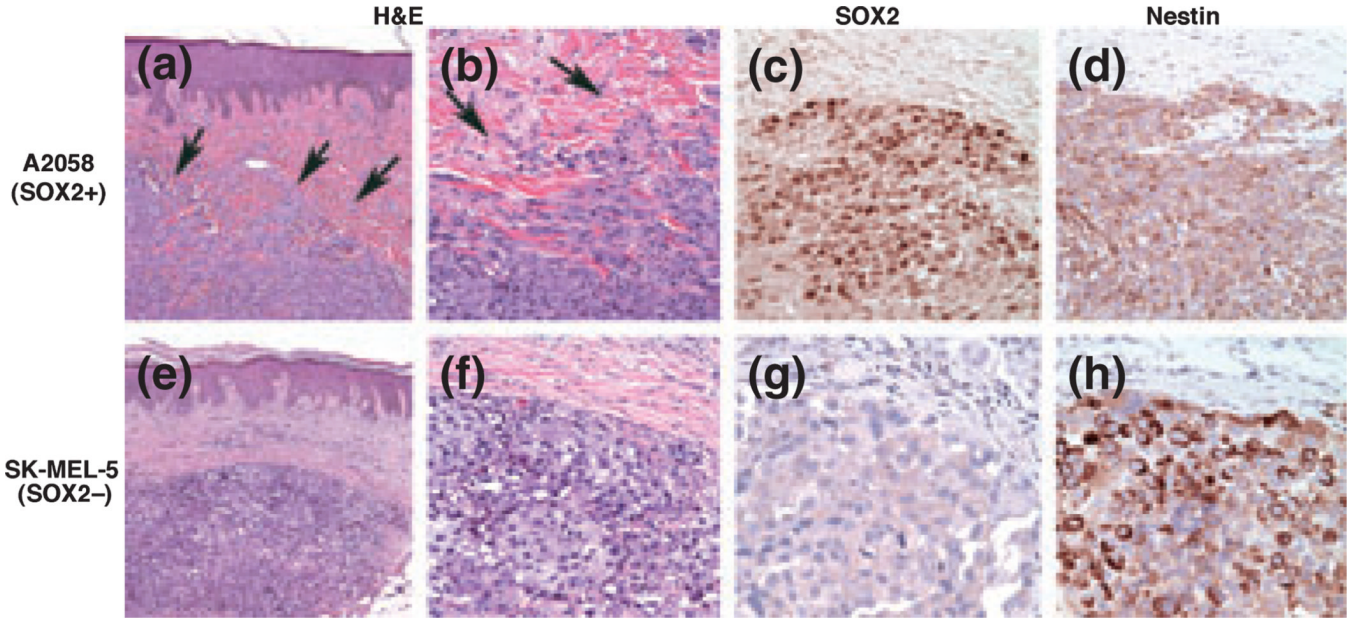

Figure 4.

SOX2 and nestin immunoreactivity in tumor xenografts grown within human dermal microenvironment of skin grafted onto immunodeficient mice. (a, b) A2058-derived tumor shows an infiltrative growth pattern (arrows) with spindle-shaped cells at the advancing edge (H&E, a: ×100; b: ×400). (c, d) The tumor is positive for SOX2 and nestin, the latter showing a peripheral pattern of immunoreactivity (c: SOX2, ×400; d: nestin, ×400). (e, f) SK-MEL-5-derived tumor showing a well-demarcated dermal tumor nodule (arrowhead = edge), which is SOX2 negative (g, ×400), with diffuse cytoplasmic nestin immunoreactivity (h, ×400).

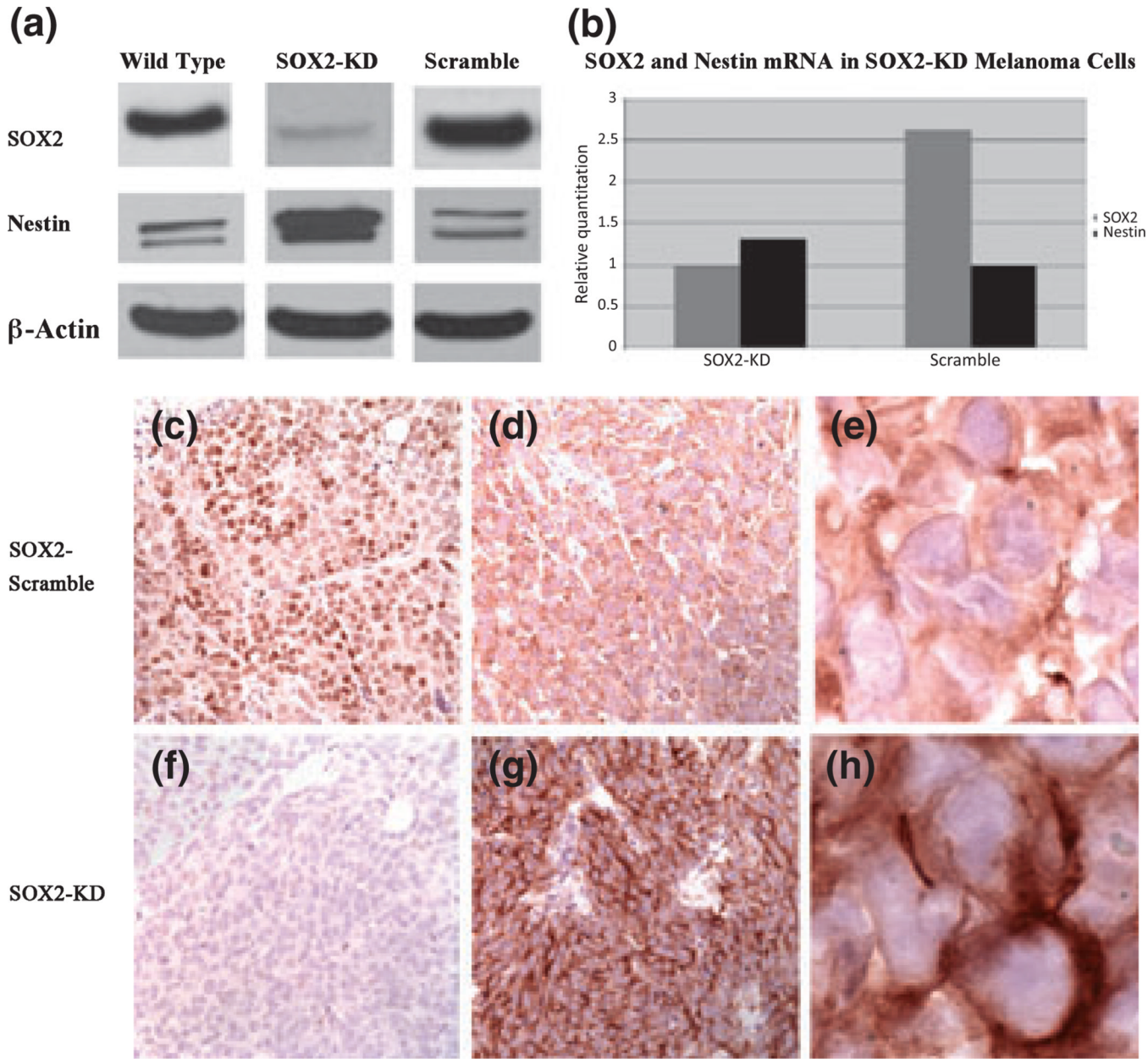

Figure 5.

SOX2 and nestin expression in A2058-SOX2-knockdown (KD) melanoma cells and correlative xenograft tumors. (a, b) A2058-SOX2-KD melanoma cells and respective xenograft tumors show decreased SOX2 and increased nestin, at both mRNA and protein levels, as compared to control A2058 cells (scramble). (c–e) Xenograft tumors derived from A2058 melanoma cells transfected with non-target shRNA (control) show strong nuclear positivity for SOX2 (c, ×100), and a peripheral distribution pattern of nestin (d, ×200; e, ×400), whereas tumors generated with A2058-SOX2-KD melanoma cells are negative for SOX2 (f, ×100), and show a diffuse cytoplasmic pattern of nestin distribution (g, ×200; h, ×400).

Table 1

SOX2 and nestin immunoreactivity in human melanocytic tumor whole sections and tissue microarrays

	Whole sections			Tissue microarrays		
	Nevi (%)	**Primary (%)**	**Metastatic (%)**	**Nevi (%)**	**Primary (%)**	**Metastatic (%)**
SOX2 only	3 (14)	0	0	1 (6)	14 (18)	3 (10)
Nestin only	0	11 (50)	2 (40)	2 (13)	18 (23)	6 (20)
SOX2 and nestin	0	10 (50)	3 (60)	1 (6)	38 (49)	21 (70)
Neither	18 (86)	0	0	12 (75)	8 (10)	0
Total	21	21 *	5	16	78	30

* One additional primary melanoma with dichotomous spindle and epithelioid cell morphology showed SOX2 positivity and a peripheral nestin pattern in the spindle cell component, whereas the epithelioid component was negative for SOX2 and exhibited diffuse cytoplasmic nestin positivity.